Lab on a Chip

Accepted Manuscript

ROYAL SOCIETY OF CHEMISTRY

www.rsc.org/loc

We present a micro-patterned silicon structure that enables the preparation of a SERS substrate and pre-concentration of the analyte molecules.

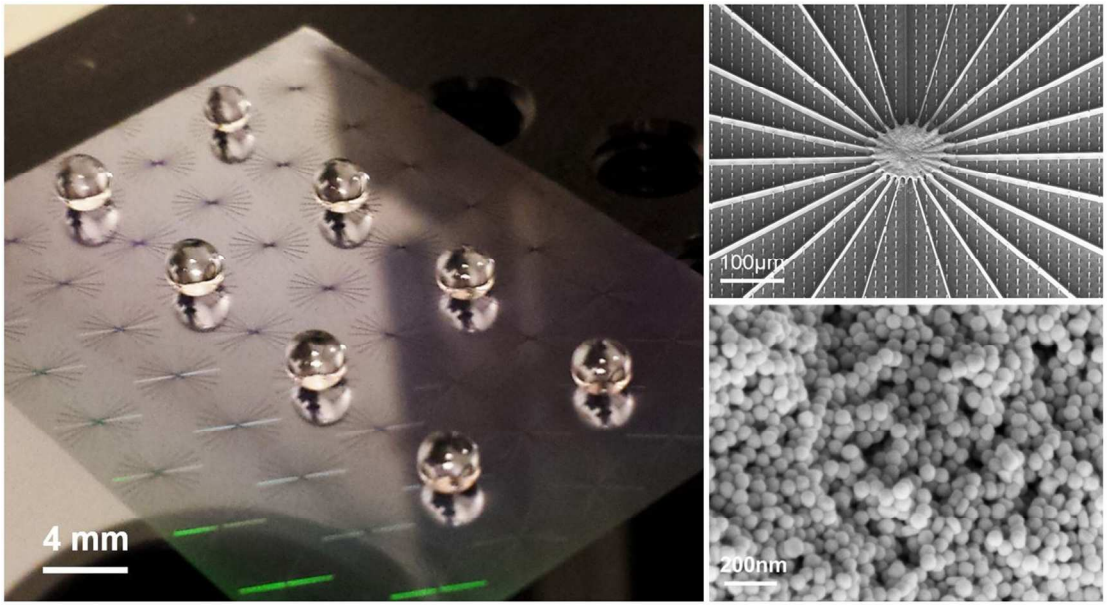

Superhydrophobic bulls-eye for surface-enhanced Raman scattering

Wuzhou Song [a], Demetri Psaltis [b] and Kenneth B. Crozier [a]

[a] School of Engineering and Applied Sciences, Harvard University, Cambridge, Massachusetts 02138, USA

[b] School of Engineering, Swiss Federal Institute of Technology Lausanne (EPFL), CH-1015, Lausanne, Switzerland

Abstract:

We present a micro-patterned silicon structure that enables the preparation of a substrate for surface-enhanced Raman scattering (SERS) as well as pre-concentration of the analyte molecules. The structure is designed to produce a hydrophobicity gradient. As a result, a water droplet placed on it will remain centred on the structure as it dries, enabling delivery of materials to its centre. The structure is therefore referred to as a superhydrophobic bulls-eye. A water droplet containing gold colloids placed on it dries to produce a cluster at the bulls-eye centre. A second water droplet placed on it, this time containing analyte molecules, dries such that the molecules are delivered to the gold colloid cluster. We demonstrate the detection of molecules at low concentrations (Rhodamine 6G at 10^{-15} M) from small droplets.

Introduction

Raman scattering enables molecules to be identified by their vibrational spectra in a label-free and multiplexed manner. Due to its inherently weak signal intensity, however, its use in sensitive molecular detection was limited until the discovery of surface-enhanced Raman scattering (SERS), a process by which the Raman scattering from molecules can be increased by factors of $\sim 10^6$ and above by chemical and electromagnetic mechanisms that occur with metal nanostructures [1]. Much of the previous work on SERS substrates has concerned novel designs and/or fabrication methods that aim to maximize electromagnetic field enhancements [2-7]. However, the strength of SERS signal depends of course not only on electromagnetic/chemical enhancement factors, but also on the number of molecules being probed. Ideally, one would like to extract all molecules in a sample to the detection region of the SERS substrate. The importance of methods for the efficient delivery of analyte molecules to the metal surfaces of SERS substrates is therefore becoming increasingly recognized [8-11]. Such methods are particularly crucial for the detection of molecules in trace quantities.

Two methods are generally employed to load analyte molecules onto prepared SERS substrates. The first involves placing the SERS substrate in a solution containing the analyte molecules for a period of time, during which the molecules diffuse to the surface and then adsorb to it. Because it relies on diffusion, however, the method is slow and inefficient in that only a very small fraction of molecules generally adsorb to the surface. Innovative variations of this method – e.g. in-situ microfluidic synthesis of colloids [12] – have been made, but the underlying challenges still remain. The second method involves placing a droplet of the analyte solution on the substrate and allowing it to dry. As SERS substrates are often metal-coated and therefore hydrophilic, however, the analyte droplet will often spread out, thereby distributing the molecules over a large area. The resultant low density of analyte molecules will therefore result in a weak SERS signal. Ideally, to detect molecules in a very dilute sample, one would like to extract all molecules in the sample to the detection region of the SERS substrate. To this end, the integration of nanofabricated SERS-active components with superhydrophobic surfaces was reported, with very low detection limits being achieved [13]. Sophisticated nanofabrication, including electron-beam lithography (EBL) and focused ion beam milling (FIB), was required to fabricate the SERS active elements and/or the structures for superhydrophobicity in the work of reference [13]. Here we present a novel Si structure in which micro-patterning produces a superhydrophobic surface with an engineered gradient of hydrophobicity. The structure is termed a superhydrophobic bulls-eye and enables preparation of both the SERS substrate, i.e. gold nanoparticle aggregate, as well as pre-concentration of the sample. The fabrication process is considerably simpler than [13], involving only optical lithography rather than EBL and FIB. Figure 1 shows the concept. The first step involves the preparation of a tiny SERS-active substrate. A water droplet containing gold colloids is pipetted onto the superhydrophobic bulls-eye. Evaporation of water in the droplet leads to the formation of a gold nanoparticle aggregate at the bulls-eye centre. In the second step, a water droplet containing the analyte is pipetted onto the same bulls-eye. Evaporation of the water in this droplet results in the analyte molecules being deposited onto the bulls-eye centre, at which the gold nanoparticle aggregate is located. In addition to the simple fabrication process, our approach requires only a very small quantity of gold, as the colloids are efficiently delivered to the SERS active region. Similarly, the efficient delivery of the analyte molecules from the droplet

to the gold nanoparticle aggregate enables them to be detected at very low concentrations by SERS. To accomplish the procedure shown in Figure 1, it is therefore essential that there be a mechanism to pin a loaded droplet to a specific position on the substrate. We here use the term "pin" to mean that when a droplet is loaded (i.e. pipetted) onto the bulls-eye, small misalignments will be corrected so that it becomes centred on the bulls-eye. The term "pin" furthermore refers to the fact that the droplet will remain centred on the bulls-eye as it dries, even in the presence of disturbances such as the substrate being tilted. In the absence of the pinning mechanism the gold colloids of the first droplet and the analyte molecules of the second droplet would not be deposited onto the same area. In addition, due to the very low adhesion force between a droplet and a superhydrophobic surface, in the absence of pinning, a droplet's position is easily disturbed after loading by substrate vibration or air currents. The superhydrophobic bulls-eye substrate we present is able to pin droplets by radial gradients of superhydrophobicity.

Device and experiments

The superhydrophobic bulls-eye is fabricated from silicon, and consists of an array of micro-pillars and radial micro-fins. A scanning electron micrograph (SEM) of the central portion of the device is shown as Figure 2. The micro-pillars are in a hexagonal lattice whose spacing is 20 μm. Each micro-pillar has a radius of 3μm and a height of 15 μm. The micro-pillars create a uniformly superhydrophobic surface. The radial micro-fins consist of 24 fins that radiate from the centre. Each fin has a width of 3 μm, a height of 15 μm, and a length of 2 mm. The entire bulls-eye therefore has a diameter of 4mm. The fins add a hydrophobicity gradient that pins droplets to the centre. In the centre of the fins, there is a circular platform with a diameter of 50 μm that acts as the deposition target for the nanoparticles or analyte molecules. The droplet pinning process can be understood using the Cassie-Baxter (C-B) model. In the C-B model, the equilibrium contact angle of liquid on an air-trapped surface can be formulated as a function of θ and γ [14]:

$$\cos\theta_{CB} = \gamma(\cos\theta + 1) - 1 \quad , \tag{1}$$

where θ_{CB} and θ are the contact angles on patterned and smooth surfaces respectively; γ is the fraction of solid surface area wetted by the liquid. This equation reveals that higher solid fractions result in smaller contact angles, i.e. less hydrophobicity. The fin structures have inherently higher solid fraction in their centre, hence creating a radial gradient of superhydrophobicity. A free standing droplet on a superhydrophobic surface has the tendency of staying in the place with lower superhydrophobicity. In our device, the fins lead to the droplet being pinned to the bulls-eye centre. Figure 3 shows the drying process of a water droplet placed on the superhydrophobic bulls-eye substrate. As water evaporates, the droplet shrinks in size while still maintaining its quasi-spherical shape and remains pinned to the centre of the radial fin pattern. During this portion of the drying process, the contact angle of the droplet remains approximately fixed at 150°. However, once the droplet reaches a diameter of ~240 μm, further drying results in sharp reductions in contact angle. This behaviour is shown in Movie 1 and Figure 1-2 of the Supplementary Material.

In order to create a radial superhydrophobicity gradient, one may alternatively consider a design consisting only of pillars, in which their spacing and/or radii are modulated. However, there are two main advantages of using the fins (with the pillars) rather than the pillar-only design. The first is that the fin design is an inherently connected structure, meaning that that there is smaller energy barrier associated with the movement of a droplet on it than on a pillar-only structure [15, 16]. The second is that the fin design has less demanding fabrication tolerance. To achieve a hydrophobicity gradient with a pillar-only structure would require sub-micron control over the variation in pillar period and/or radius with position on the substrate. This level of control is difficult to achieve with the laser lithography tool employed in this work.

Fabrication starts with the coating of positive photoresist on a silicon wafer. The post and fin patterns are then patterned with a laser lithography system (Heidelberg DWL200). After resist development, anisotropic deep reactive ion etching is performed (Alcatel 601E). We next remove the photoresist with an oxygen plasma. To render the silicon surface hydrophobic, a self-assembled monolayer (SAM) of 1,1,-2,2,-tetrahydroperfluorodecyltrichlorosilane is deposited on the substrate by vapour phase deposition in a vacuum chamber followed by immediately baking it in the oven at 150° for 1 hour to remove the excess organic molecules [15]. The step is critical in order to form the desired SAM on the silicon surface without contamination.

We next create a SERS active site on the device. This involves the use of gold colloids that are cleaned as follows. A gold colloid solution containing ~10^{10} particles/ml is purchased from BBI Solutions Inc. The nanoparticles are nano-spheres with diameters that average 60 nm. The solution is centrifuged at 1000 rpm for 15 minutes. The nanoparticles are then extracted and added to pure water, with the resultant mixture placed in an ultrasonic bath for several minutes. This process is repeated five times or more. A droplet of pure water containing the cleaned gold colloids is then pipetted onto the fin pattern. The initial volume and radius of the droplet are 20 μL and ~800 μm, respectively. Figure 4 (a) shows a SEM image of central portion of the device after the drying process is complete. The nanoparticles are densely aggregated in a circular region with a diameter of ~100 μm. An SEM image of the aggregated gold nanoparticles obtained at a higher magnification is shown as Figure 4(b). It is likely that considerable electromagnetic field enhancement occurs in the regions where the particles contact one another [17]. We note that while we did not take steps to control inter-particle spacing, this could be achieved in the future using various techniques, e.g. by forming ultra-thin silica shells on the gold particles [18].

At this point, the chip can be used for SERS. As the gold colloid aggregate is in dry form, the substrate is expected to have a much longer shelf life than gold colliods in solution. A droplet of R6G aqueous solution is pipetted onto the bulls-eye. The volume of the droplet is also 20μL. We observe that the droplet is pinned to the centre of the bulls-eye, at which the gold nanoparticle aggregate is located. As the droplet dries, the concentration of R6G increases continually. At the end of the process, i.e. after the droplet is fully dried, the R6G molecules originally in the droplet have been deposited on the gold nanoparticle aggregate at the bulls-eye centre. We next measure SERS spectra. The experimental observation and results are discussed in the following section.

Results and discussion

SERS spectra are measured using a commercial Raman microscope (Horiba Jobin Yvon LabRAM) using an excitation laser with a wavelength of 532 nm. The excitation laser power is 0.24 mW. An objective lens with a numerical aperture (NA) of 0.75 and a magnification of 50× is used. The acquisition time is 30 seconds. To evaluate the capabilities of this method for trace detection, we measure a series of R6G aqueous solutions with concentrations ranging from 10^{-10} M to 10^{-15} M. The best result at each concentration is shown in Figure 5, where the Raman signal is normalized to the excitation laser power and acquisition time. The base line correction function of the Raman microscope software package has been applied to all spectra of Figure 5 to remove the fluorescent background signal. It can be seen that even down to concentrations of 10^{-15} M, the main Raman peak of the spectrum at 1361 cm^{-1} can be still observed. The results of Figure 5 are re-plotted as Supplementary Figure 3, with the intensities of several SERS lines shown as a function of the concentration of R6G in the droplet. It can be seen that the SERS intensities increase with concentration.

An essential ingredient of our method is that the droplet should be pinned to a specific point on the substrate in order for the analyte molecules from the second droplet be deposited at the same location as the gold colloids from the first droplet. To confirm that this is achieved, we take bright-field (Supplementary Figure 4a) and fluorescence (Supplementary Figure 4b) microscope images of the superhydrophobic bulls-eye after the gold colloid and R6G droplets are applied and dried. The dark spot in the centre of the bright-field image represents the gold colloid aggregate. The fluorescence image is captured with a colour charge coupled device (CCD) camera with a light emitting diode (LED) excitation source centred at a wavelength of 515 nm. A long pass filter with cut-off wavelength at 520 nm is used as the emission filter. It can be seen that the bright spot in the fluorescence image, indicating the presence of R6G, has an extent that is commensurate with the dark area of the bright-field image. This indicates the R6G molecules are deposited onto the gold colloid aggregate as desired.

To further investigate the benefit from the superhydrophobic bulls-eye substrate, we consider an alternative substrate for SERS consisting of a flat silicon wafer coated with a monolayer of 1,1,-2,2,-tetrahydroperfluorodecyltrichlorosilane to make the surface hydrophobic. We perform the same steps as before, applying one droplet containing gold colloid and another containing R6G. The bright-field and fluorescence images of the substrate after these droplets have been applied are shown as Supplementary Figure 5a and 5b, respectively. It can be seen that both the gold particles and the R6G molecules are deposited over a large surface area and in a very random manner. This is in contrast with the superhydrophobic bulls-eye substrate, for which the gold colloid and R6G are largely deposited into a small circular region with a diameter of ~100 μm.

The superhydrophobic bulls-eye offers considerable benefits over a regular superhydrophobic surface is terms of placing and maintaining a droplet at a specific location. We performed experiments on a regular superhydrophobic surface (silicon pillars and SAM, but no micro-fins) but found that in most cases, after being pipetted, droplets would move quickly to the edge of the substrate, unless steps had been taken to make the substrate level. Furthermore, even

if the substrate were level during the drying process, small perturbations such as table vibration and/or air flow would lead to the droplet being displaced. By contrast, under both ideal (i.e. substrate is level and no mechanical perturbations) and non-ideal conditions, the superhydrophobic bulls-eye offers benefits in placing and maintaining a droplet at a specific location. In Figure 6 of the Supplementary Material, we demonstrate that an array of superhydrophobic bulls-eyes permits us to form a regular array of droplets (2×4) by hand pipetting. This would be very difficult to achieve with a regular superhydrophobic surface due to the factors discussed above. The robustness to mechanical perturbation is further illustrated in Movies 2 and 3 of the Supplementary Material that show the result of tilting a superhydrophobic bulls-eye device and a regular superhydrophobic device, respectively. It can be seen that a droplet remains on a superhydrophobic bulls-eye even as it is tilted by a few degrees. By contrast, the droplet readily moves with the tilting of the regular superhydrophobic surface.

Conclusion

In summary, we developed a novel method for both SERS substrate preparation and sample preconcentration based on a micro-engineered superhydrophobic bulls-eye. Via its hydrophobicity gradient, the bulls-eye permits nanoparticles or molecules from a droplet to be guided to a particular target position during the evaporation process. We show that this permits highly sensitive SERS spectroscopy to be carried out on samples that have very small volumes and contain analyte molecules at very low concentrations. We demonstrate SERS spectra from water droplets containing R6G at concentrations down to 10^{-15} M. Our method furthermore uses only a very small quantity of gold, which is advantageous from a practical standpoint due to the high cost of this material. The bulls-eye is fabricated by photolithography in this report, but we anticipate that other materials and imprinting technologies could be employed in future in order to further significantly reduce the cost [19, 20]. Based on its low cost, high sensitivity, and compatibility with very small sample volumes, we expect the method we introduce could find important applications in the trace detection of chemicals.

Acknowledgements

W. Song acknowledges the “Swiss National Science Foundation” for providing his postdoctoral fellowship under the program of “Early postdoc. Mobility”.

References

[1] P. L. Stiles, J. Dieringer, N. Shah and R. Van Duyne, Annu. Rev. Anal. Chem., 2008, **1**, 601-626.

[2] Y. Chu, M. G. Banaee and K. B. Crozier, ASC Nano, 2010, **4** (5), 2804-2810.

[3] D. Wang, W. Zhu, M. Best, J Camden and K. Crozier, Nano Lett., 2013, **13**, 2194-2198.

[4] J. Parisi, L. Su and Y. Lei, Lab Chip, 2013, **13**, 1501-1508.

[5] E. Chung, R. Gao, J Lo, N. Choi, D. W. Lim, E. K. Lee, S. Chang and J. Choo, Lab Chip, 2013, **13**, 260-266.

[6] Y. Guo, M. K. Khaing Oo, K. Reddy and X. Fan, ACS Nano, 2012, **6**, 381-388.

[7] A. W. Clark, A. Glidle, D. R. S. Cumming and J. M. Cooper, Appl. Phys. Lett., 2008, **93**, 023121.

[8] H. Cho, B. Lee, G. Liu, A. Agarwal and L. P. Lee, Lab Chip, 2009, **9**, 3360-3363.

[9] P. D. Lacharmoise, E. C. Le Ru and P. G. Etchegoin, ACS Nano, 2009, **3**, 66-72.

[10] C. Escobedo, A. G. Brolo, R. Gordon and D. Sinton, Nano Lett., 2012 **12**, 1592-1596.

[11] I. Choi, Y. S. Huh and D. Erickson, Lab on a Chip, 2011, 11, 632-638.

[12] R. Wilson, S. A. Bowden, J. Parnell and J. M. Cooper, Anal. Chem., 2010, **82** 2119-2123.

[13] F. De Angelis, F. Gentile, F. Mecarini, G. Das, M. Moretti, P. Candeloro, M. L. Coluccio, G. Cojoc, A. Accardo, C. Liberale, R. P. Zaccaria, G. Perozziello, L. Tirinato, A. Toma, G. Cuda, R. Cingolani and E. Di Fabrizio Nat. Photonics, 2011, **5**, 682-687.

[14] A.B.D. Cassie, S. Baxter, Trans. Faraday Soc., 1944, **40**, 546–551

[15] X. Chen, R. Ma, J. Li, C. Hao, W. Guo, B. L Luk, S. C. Li, S. Yao and Z. Wang, Phys. Rev. Lett., 2012, **109**, 116101.

[16] J. T. Yang, J. C. Chen, K. J. Huang and J. A. Yeh, J. Microelectromechanical System, 2006, **15** (3), 697-707.

[17] A. M. Schwartzberg, C. D. Crant, A. Wolcott, C. E. Talley, T. R. Huser, R. Bogomolni and J. Z. Zhang, J. Phys. Chem. B, 2004, **108**, 19191-19197.

[18] A. Vanderkooy, Y. Chen, F. Gonzaga and M. A. Brook, ACS Appl. Mater. Interfaces, 2011, **3**, 3942-3947.

[19] A. Pozzato, S. D. Zillo, G. Fois, D. Vendramin, G. Mistura, M. Belotti, Y. Chen and M. Natali, Microelectronic Engineering, 2006, **83**, 884-888

[20] T. Kobayashi, K. Shimizu, Y. Kaizuma and S. Konishi, Appl. Phys. Lett., 2011, **98**, 123706.

Captions

Figure 1: Operating principle of engineered superhydrophobic substrate for preparing SERS-active region (a, b) and concentrating the sample (c, d).

Figure 2: Scanning electron microscope (SEM) image of centre area of superhydrophobic bulls-eye

Figure 3: Photographs of a droplet (side view) as it dries on a superhydrophobic surface.

Figure 4: (a) SEM image of superhydrophobic bulls-eye after gold colloid droplet has dried on it; (b) SEM image of gold colloid aggregate at bulls-eye centre.

Figure 5: SERS spectra measured from bulls-eye after drying of droplets containing R6G at concentrations from 10^{-10} M to 10^{-15} M.

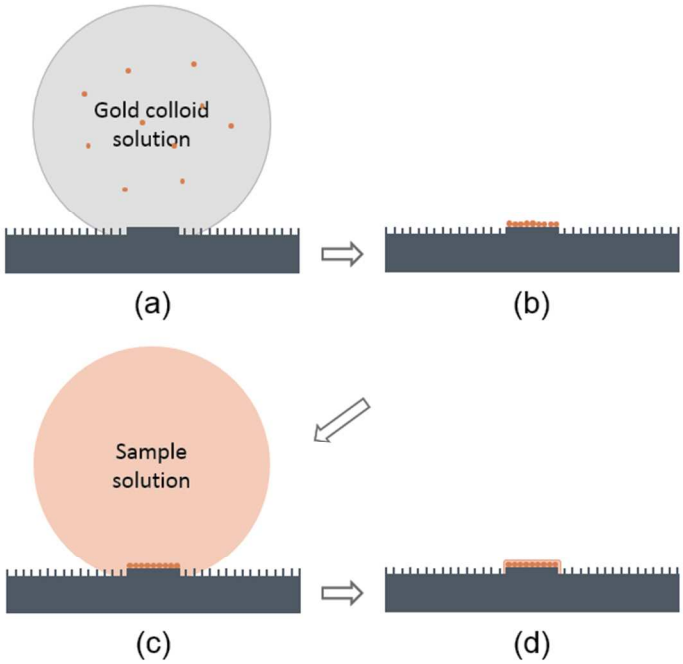

Figure 1

Figure 2

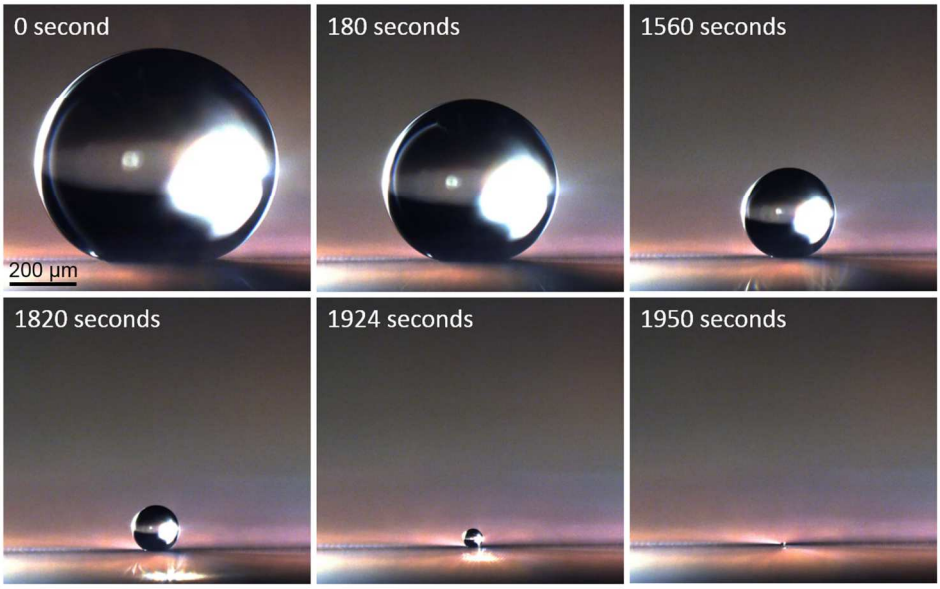

Figure 3

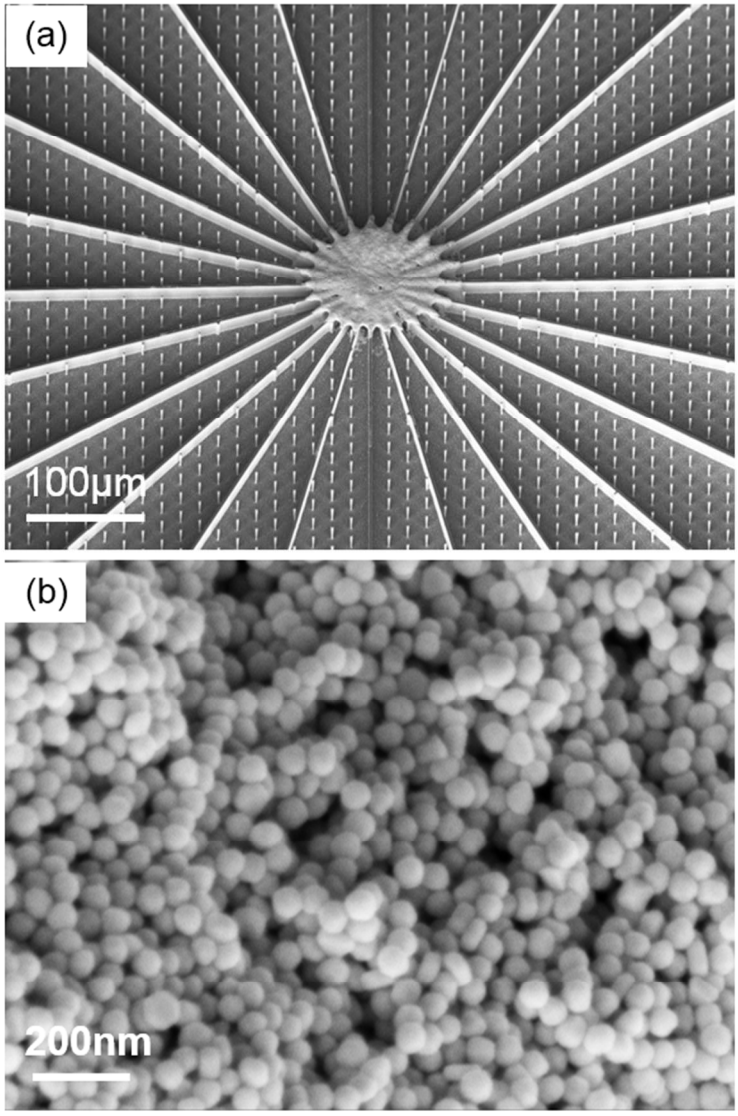

Figure 4

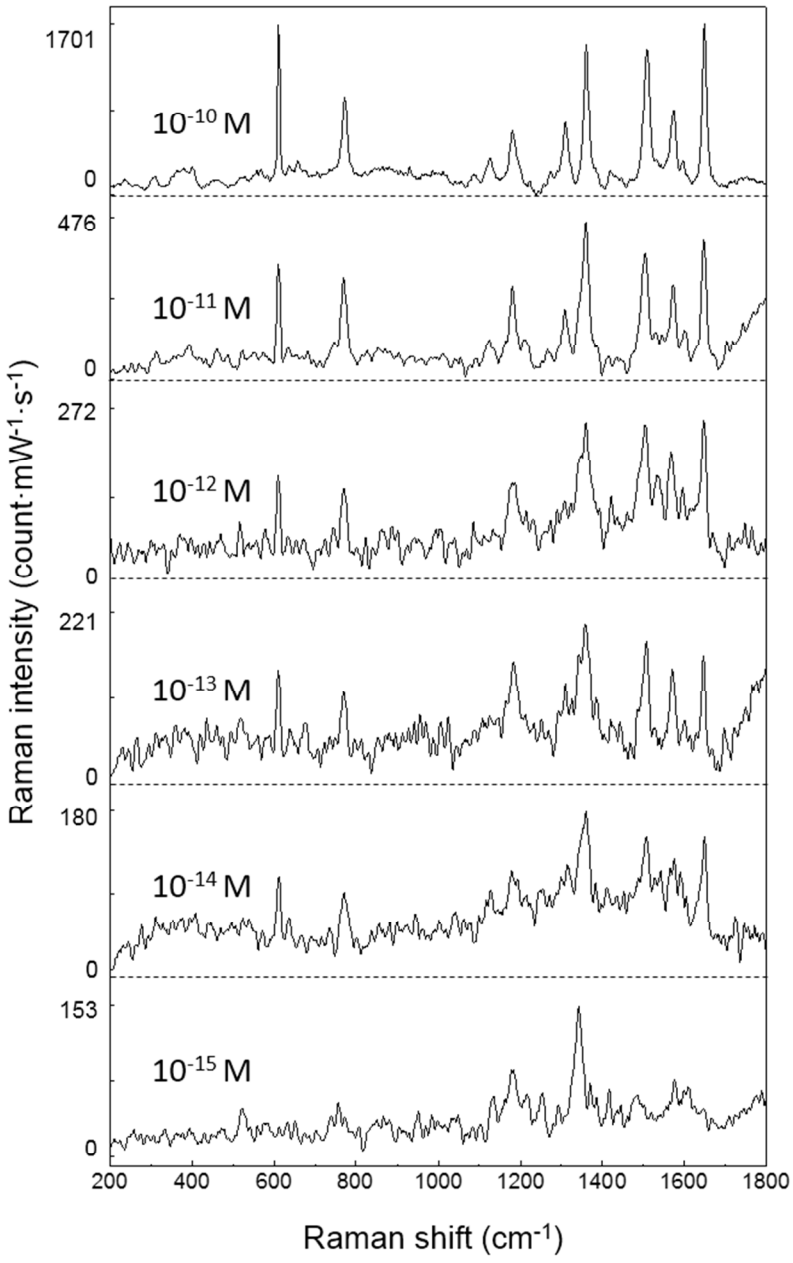

Figure 5